Article

Discovery Medicine 2024; 36(186): 1386–1397
https://doi.org/10.24976/Discov.Med.202436186.129

Effects of IL-6R Expression on IL-6/STAT3/HIF-1α Signaling Pathway in a Mouse Model of Parkinson's Disease with Type 2 Diabetes Co-Morbidity

Aiping Hu[1,2], Yuqing She[2], Yang Wang[2], Xue Cao[2], Ran Li[2], Jing Wang[2], Lizhi Yu[3], Haifeng Jiang[3], Yang Zhao[1,4,*]

[1]Nanjing University of Chinese Medicine, 210023 Nanjing, Jiangsu, China
[2]Department of Endocrinology, Nanjing Pukou People's Hospital, 211800 Nanjing, Jiangsu, China
[3]Department of Neurology, Nanjing Pukou People's Hospital, 211800 Nanjing, Jiangsu, China
[4]Department of Neurology, Nanjing Hospital of Chinese Medicine Affiliated to Nanjing University of Chinese Medicine, 210012 Nanjing, Jiangsu, China
*Correspondence: yangzhaotcm@njucm.edu.cn (Yang Zhao)
Published: 20 July 2024

Background: More and more evidence has shown the process of Parkinson's disease (PD). Probably, inflammation exerts a crucial role between them. Therefore, the aim of this study was to analyze the impact of interleukin-6 receptor (IL-6R) expression on the IL-6/signal transducer and activator of transcription 3 (STAT3)/hypoxia-inducible factor-1α (HIF-1α) inflammatory signaling pathway within a mouse model of PD with type 2 diabetes mellitus (T2DM) as co-morbidity.

Methods: We chose healthy wild-type C57BL/6J male mice at the age of 10 weeks to prepare a mouse model of PD with T2DM co-morbidity. Adeno-associated virus (AAV) overexpressing *IL-6R* or AAV *IL-6R*-shRNA genes were injected into the substantia nigra (SN) of the mice. The behavioral indices of the pole test were used for examining the motor function of the mice. Using immunofluorescence analysis, the impacts of IL-6R on the level of tyrosine hydroxylase (TH) and anti-ionized calcium-binding adaptor molecule 1 (IBA-1) on dopaminergic neurons and microglia were examined. Additionally, enzyme-linked immunosorbent assay (ELISA) was adopted for determining the expressions of HIF-1α and inflammatory cytokines like tumor necrosis factor-α (TNF-α), IL-1β, IL-6, and IL-4 in the serum. In this study, the protein expression levels of TH, α-Synuclein (α-Syn), IBA-1, IL-6, IL-6R, phosphorylated and total signal transducer and activator of transcription 3 (p-STAT3 (Tyr705) and STAT3) and HIF-1α in the SN were tested via western blotting. To ascertain the mRNA expressions of *TNF-α*, *IL-1β*, *IL-6*, *IL-4*, and *HIF-1α*, we used quantitative Real-Time Polymerase Chain Reaction (RT-qPCR).

Results: *IL-6R*-shRNA treatment could markedly shorten the total time of PD in the T2DM co-morbidity mouse model based on the pole test results, reverse the decrease in TH-positive neurons stimulated by 1-Methyl-4-phenyl-1,2,3,6-tetrahydropyridine hydrochloride (MPTP), and lower the activation of microglia (all $p < 0.05$). Further, *IL-6R*-shRNA treatment hindered the expression of IL-6, p-STAT3 (Tyr705), and HIF-1α in the SN, lowered the levels of TNF-α, IL-1β, IL-6, IL-4, and HIF-1α in the serum, and mRNA expressions of *TNF-α*, *IL-1β*, *IL-6*, and *HIF-1α* in the SN (all $p < 0.05$). In contrast, IL-6R overexpression reduced TH levels, upregulated the level of IBA-1, IL-6, p-STAT3 (Tyr705), and HIF-1α, increased the level of IL-1β, TNF-α, IL-6, IL-4, and HIF-1α (all $p < 0.05$) in the serum and SN in the PD mouse model with T2DM as a co-morbidity.

Conclusions: PD progression with T2DM as a co-morbidity can be boosted by AAV IL-6R-overexpression through upregulation of the IL-6/STAT3/HIF-1α axis. Conversely, AAV *IL-6R*-shRNA treatment suppressed the IL-6/STAT3/HIF-1α pathway and alleviated neuroinflammation, thus weakening the development of PD with T2DM as a co-morbidity.

Keywords: Parkinson's disease; type 2 diabetes mellitus; IL-6/STAT3/HIF-1α pathway; IL-6R-overexpression; *IL-6R*-shRNA; neuroinflammation

Introduction

Parkinson's disease (PD) and type 2 diabetes mellitus (T2DM) mean aging disorders. PD refers to a neurodegenerative disorder where dopaminergic (DA) neurons are deprived and the abnormal accumulation of α-Synuclein (α-Syn) protein forms Lewy bodies [1]. T2DM refers to a chronic metabolic disease featured by the dysfunction of β-cells and insulin resistance [2]. Hong *et al.* [3] reported that T2DM patients show a greater risk of developing PD. Even though the pathogenesis of PD has not yet been explained, emerging evidence suggests a biological relationship between PD and T2DM. These disorders involve several overlapping mechanisms such as aberrant protein accumulation, lysosomal and mitochondrial dysfunction, as well as chronic systemic inflammation [4].

Neuroinflammation has a vital effect on the pathogenesis and development of PD. Microglia can enter an activated inflammatory state after stimulation with lipopolysaccharide and show elevated levels of pro-inflammatory factors like tumor necrosis factor-α (TNF-α), interleukin (IL)-1β, and IL-6, which triggers neuroinflammation [4]. Microglial activation and inflammation have been found in humans and rats with T2DM [5,6]. Van *et al*. [7] showed that the presence of metabolic inflammation triggered by T2DM tends to elevate the production of inflammatory cytokines in the brain by disrupting the blood-brain barrier (BBB). T2DM aggravates neuroinflammation in patients with PD. As a result, a better influence on the impact of inflammation on PD and T2DM can offer novel perspectives on the underlying pathological processes and contribute to the establishment of effective therapeutic methods. Our study aimed to establish a mouse model of PD with T2DM co-morbidity *in vivo* with C57BL/6 mice and investigate the potential associated inflammatory mechanisms involved.

Materials and Methods

Animals

The involved experiments were carried out on male C57BL/6J mice who were ten weeks of age (weighing 25–30 g). Seventy C57BL/6J mice were provided by Cyagen Biosciences Inc. (Suzhou, China) and were offered food and water *ad libitum* in clean cages lined with sawdust, based on standard housing conditions (12/12 h light/dark cycle, 22 $\pm$ 2 °C, and 55 $\pm$ 5% humidity). Animals were maintained as per the instructions of the revised Animals (Scientific Procedures) Act of 1986 in the United Kingdom. The approval of the experimental protocols was provided by the Experimental Animal Ethics Committee of the Nanjing University of Chinese Medicine (ethical approval number ACU220604). All surgeries in this study were performed under anesthesia with 0.3% pentobarbital sodium, and the dose was based on animal weight (50 mg/kg). Steps were taken to minimize animal suffering, and the procedures were guided following the guidelines of the American Veterinary Medical Association.

Experimental Groups

Before the experiments, 70 mice were acclimatized in the animal facility for seven days and subsequently randomly assigned to seven groups, each group including 10 mice, based on the random number table method as follows:

Normal Control (NC) group: Mice were fed regular chow (including 5% fat) and water.

PD group: Mice were fed regular chow (including 5% fat) and injected intraperitoneally with 1-Methyl-4-phenyl-1,2,3,6-tetrahydropyridine hydrochloride (MPTP) (30 mg/kg) at 10:00 AM for 9 days [8], starting on the same day as the PD+T2DM group with the first MPTP injection.

PD+T2DM group: Mice were fed a high-fat diet (HFD) (including 30% fat) for 8 weeks and subsequently injected intraperitoneally with streptozotocin (STZ; 30 mg/kg) at 10:00 AM for 5 days [9,10]. Three days after injection, the mice were fasted for 12 hours. Afterwards, we measured fasting blood glucose levels. Mice with fasting blood glucose concentrations of $>$250 mg/dL were regarded to be diabetic [9]. These mice were subsequently injected intraperitoneally with MPTP (30 mg/kg) at 10:00 AM for 9 days. Injections continued until the pole test was performed to confirm motor dysfunction, and the day on which an obvious decrease was found in the pole test was considered the day of PD model development (9th day after the first injection).

Adeno-associated virus (AAV) vector carrying IL-6R-overexpression negative control+PD+T2DM (IL-6R-OE-NC+PD+T2DM) group: The mice were fed an HFD for 7 weeks. An AAV carrying interleukin-6 receptor (IL-6R)-overexpression no load RNA was injected into the left substantia nigra (SN). These mice continued to be fed an HFD. One week later, the same conditions as the PD+T2DM group were maintained.

AAV vectors carrying the *IL-6R*-overexpression target gene+PD+T2DM (IL-6R-OE+PD+T2DM) group: The mice were fed an HFD for 49 days. An AAV carrying the *IL-6R*-overexpression target gene was injected into the left SN. Then, the mice continued to be fed an HFD. One week later, the conditions were maintained the same as those in the PD+T2DM group.

AAV vector carrying *IL-6R*-shRNA negative control+PD+T2DM (*IL-6R*-shRNA-NC+PD+T2DM) group: Mice were fed an HFD for 7 weeks. AAV carrying *IL-6R*-shRNA no load RNA was injected into the left SN. Subsequently, the mice were continued to be fed an HFD. One week later, the same conditions as the PD+T2DM group were maintained.

AAV vector carrying the *IL-6R*-shRNA target gene+PD+T2DM (*IL-6R*-shRNA+PD+T2DM) group: Mice were fed an HFD for 7 weeks. AAV carrying the *IL-6R*-shRNA target gene was injected into the left SN. The mice were continued to be fed an HFD. One week later, the same conditions as the PD+T2DM group were maintained.

Animal modeling methods are shown below in Fig. 1.

Equipment and Reagents

In this study, a frozen microtome (RM2016, Leica Biosystems, Wetzlar, Germany), stereotaxic brain apparatus (DB053, Beijing Zhishuduobao Biological Technology Co., Ltd., Beijing, China), fluorescence microscope (Nikon Eclipse C1, Nikon, Tokyo, Japan), electrophoresis apparatus (Mini Protean 3, BioRad, Hercules, CA, USA) and transfer machine (170-3930, Bio-Rad, Hercules, CA, USA), and a 1 µL micro-syringe (O31/0113000236C001-2017, Shanghai Gaoge Industry

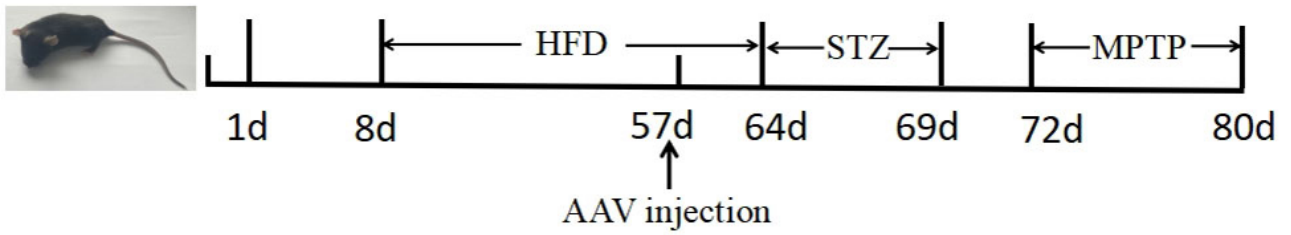

Fig. 1. Animal modeling process. HFD, high-fat diet; STZ, streptozotocin; MPTP, 1-Methyl-4-phenyl-1;2;3;6-tetrahydropyridine hydrochloride; AAV, adeno-associated virus; d, day.

and Trade Co., Ltd., Shanghai, China) were used. *IL-6R*-shRNA and *IL-6R* overexpressing plasmids were designed and constructed by Genechem Corporation (Shanghai, China). The coding sequence of the *IL-6R*-shRNA was CGAAGCGTTTCACAGCTTAAA. The coding sequence of the *IL-6R* overexpression plasmids is included in the **Supplementary Materials** section. MPTP (S31504) was purchased from Yuanye Biotechnology Co., Ltd. (Shanghai, China). STZ (S0130) was purchased from Sigma-Aldrich (St. Louis, MO, USA). Anti-IL-6 (ab290735), anti-IL-6R (ab300581), anti-signal transducer and activator of transcription 3 (STAT3) (ab109085), anti-phospho-STAT3 (ab76315), and anti-ionized calcium-binding adaptor molecule 1 (IBA-1) antibodies (ab178847) were bought from Abcam, UK. The anti-hypoxia-inducible factor-1α (HIF-lα) (14179S), anti-Glyceraldehyde 3-phosphate dehydrogenase (GAPDH) (5174S), anti-α-Synuclein (4179S), and anti-tyrosine hydroxylase (TH) (2792S) antibodies were purchased from Cell Signalling Technology (Danvers, MA, USA). The secondary antibody applied was horseradish peroxidase (HRP)-labeled goat anti-rabbit IgG (A0208, Shanghai Beyotime Biotechnology Co., Ltd., Shanghai, China). In addition, the TNF-α (AF2132-A), IL-1β (AF2040-A), IL-6 (AF2163-A), IL-4 (AF2165-A), hypoxia-inducible factor-1α (HIF-1α) (AF2393-A), and Insulin ELISA Kits (AF2579-A) were purchased from Hunan Aifang Biotechnology Co., Ltd., Changsha, China. The source of additional reagents and instruments include SYBR® Premix Ex Taq (RR820A, Takara, Osaka, Japan), the PrimeScript™ RT reagent Kit with gDNA Eraser (RR820A, Takara, Osaka, Japan), Trizol (9108, Takara, Osaka, Japan), nucleic acid analyzer (Thermo, Waltham, MA, USA), and quantitative real-time PCR instrument (Applied Biosystems 7500, Thermo, Waltham, MA, USA).

Stereotaxic Injection

Mice were anesthetized with 0.3% pentobarbital sodium and firmly fixed on a stereotactic device, after which the scalp was cut midsagittal to expose the bregma. In accordance with the stereotaxic map of the mouse brain, the coordinates compared with the bregma of the left SN included: antero-posterior (AP)—3.0 mm; medial-lateral (ML)—1.3 mm; dorsoventral (DV)—4.7 mm. The control or AAV (0.3 µL) which carried the target gene was injected with a micro-syringe into the left SN of mice in a drilled microwell in the skull. With the injection being performed, the needle was left in place for 5 min and subsequently slowly removed from the brain to prevent reflux. The mice were observed for wound healing and recovery after surgery.

Pole Test

The pole test is used for evaluating bradykinesia and motor coordination in mice and was carried out the day after the last intraperitoneal MPTP injection. According to the protocol of Chen *et al.* [11], a PV tube with a length of 55 cm and a diameter of 1 cm was chosen. With the purpose of preventing the mice from skidding, the outside of the pole was closely wrapped with white tape. A ball (2 cm diameter) was fixed on top of the pole on a plastic foam base and positioned in a cage with a thick dressing. The mice were positioned on the upper side of the spherical protrusions and the time taken by the head to turn down (T-turn) and the total time (T-total) taken to climb to the bottom were recorded. Every mouse was examined twice with an interval of 2 min between every test. The average value from the results of both tests was obtained.

Immunofluorescence and Quantitative Analyses

After the pole test, all the mice were anesthetized with 0.3% pentobarbital sodium and the amount of anesthesia was 50 mg/kg. They were euthanized with a cervical dislocation after anesthesia and removal of brain tissue. Three mice from each group were chosen for immunofluorescence analysis randomly. The brains of the mice were quickly removed and then fixed at 4 °C overnight with 4% polyformaldehyde after perfusion with normal saline into the left ventricle. Next, the brain tissue was incubated with a 20% sucrose solution, dehydrated with a 30% sucrose solution, and embedded in OCT gel. Afterwards, the brain tissue was cut into 20 µm thick coronal slices at –20 °C. Slices were subjected to incubation overnight at 4 °C with anti-TH (1:5000) or anti-IBA-1 (1:100) antibodies. On the second day, the slices were rinsed using PBS and subject to incubation with a secondary goat anti-rabbit IgG antibody (1:300) under the condition of room temperature in the dark for an hour, rinsed three times with PBS (5 min washes),

and air-dried under dark conditions. DAPI was used for staining the nuclei. To obtain the images, a fluorescence microscope was applied. ImageJ 1.51j8 software (National Institutes of Health, Bethesda, MD, USA) was adopted for counting the number of TH-positive neurons and activated microglial cells in parallel brain sections.

Western Blotting and Quantitative Analysis

The mice were decapitated for brain tissue extraction, and proteins from the SN tissues were extracted by homogenization at 12,000 rpm for 10 min with the addition of a protease inhibitor cocktail (P8340, Sigma, St. Louis, MO, USA) and a phosphatase inhibitor (P0044, Sigma, St. Louis, MO, USA) to obtain lysates. Protein expression was evaluated by western blotting. Protein concentrations were identified with the use of the BCA assay (Shanghai Beyotime Biological Co., Ltd., Shanghai, China).

Concentrated and separated gels were prepared in line with the guidance of the manufacturer. The proteins were separated by 6%–10% SDS-PAGE gels (80 V, 0.5 h; subsequently 120 V, 1 h), followed by transfer onto a 0.22 µm polyvinylidene difluoride (PVDF) membrane. The membranes were blocked with the concentration of 5% BSA for 60 min and incubated using the primary antibodies including anti-IBA-1 (1:1000), anti-HIF-1α (1:1000), anti-IL-6 (1:1000), anti-IL-6R (1:1000), anti-STAT3 (1:1000), anti-p-STAT3 (1:2000), anti-TH (1:1000), anti-α-Syn (1:1000), and anti-GAPDH (1:1000) at 4 °C, overnight. The following day, HRP peroxidase-conjugated secondary antibodies (goat anti-rabbit IgG, 1:5000) were supplemented to the membranes for an hour at room temperature. Using Tris-buffered saline and Tween 20 (TBST), the membranes were rinsed three times (10 min each). In addition, protein bands were visualized by chemiluminescence (ECL) (180-5001, Shanghai Tanon Science & Technology Co., Ltd., Shanghai, China). All the experiments were repeated three times. ImageJ 1.51j8 software was employed to explore the density of each protein band.

Enzyme-Linked Immunosorbent Assays

Before sacrifice with a cervical dislocation, the mice were fasted for 12 hours. Blood from each mouse (1 mL) was obtained and exposed to centrifugation at 3000 rpm at 4 °C for 10 min. The serum was preserved at –80 °C. The levels of insulin (ISN), HIF-1α, and inflammatory factors which included TNF-α, IL-6, IL-4, and IL-1β were evaluated as per the ELISA kit instructions.

Fasting Blood Glucose Level Measurements

The mice were fasted for 12 hours before sacrifice. After serum isolation, blood glucose levels were analyzed based on a Blood Glucose Analysis Kit (Contour TS 1816, Bayer, Leverkusen, Germany) in line with the guidance of the manufacturer.

Quantitative Real-Time Polymerase Chain Reaction (RT-qPCR)

Total RNA was extracted from frozen tissue samples of the SN with TRIzol reagent. Then, a nucleic acid analyzer was used to identify RNA concentration and purity. After removing genomic DNA, the RNA was reverse transcribed with the PrimeScript™ RT kit (with gDNA eraser). The SYBR Premix Ex Taq II kit was adopted for analyzing mRNA expression levels of target genes with RT-qPCR. The thermocycling conditions used were 95 °C for 20 seconds, followed by 40 PCR cycles with denaturation at 95 °C for 3 seconds and an extension at 60 °C for 30 seconds. To determine the purity of the PCR products, melt curves were obtained at the end of each cycle. The mRNA levels of the target genes were normalized to those of GAPDH within the same sample. According to the $2^{-\Delta\Delta Ct}$ formula, the expressions of target genes were calculated. Then, Table 1 lists the primer sequences for RT-qPCR.

Statistical Analysis

All analyses were carried out based on IBM SPSS Statistics for Windows version 22.0 (IBM Corp., Armonk, NY, USA) and GraphPad Prism 8 (GraphPad Software, Inc., San Diego, CA, USA). Data showing a normal distribution are plotted as the mean $\pm$ standard deviation (SD). In addition, one-way ANOVA was adopted for comparing multiple groups, and the Bonferroni correction test was adopted for post-hoc analysis. $p < 0.05$ was indicated to be of statistical significance.

Results

Impact of IL-6R Expression on Pole Test Results in Parkinson's Disease Comorbid Type 2 Diabetes Mice

This study evaluated the balance and coordination ability of mice using the pole test. Comparatively, the return time of mice in the PD, PD+T2DM, IL-6R-OE-NC+PD+T2DM, IL-6R-OE+PD+T2DM, *IL-6R*-shRNA-NC+PD+T2DM, and *IL-6R*-shRNA+PD+T2DM groups were observed to be higher ($p < 0.05$, $p < 0.01$, $p < 0.05$, $p < 0.01$, $p < 0.01$, and $p < 0.05$, respectively). In addition, the total time was markedly longer in the PD, PD+T2DM, IL-6R-OE-NC+PD+T2DM, IL-6R-OE+PD+T2DM, *IL-6R*-shRNA-NC+PD+T2DM, and *IL-6R*-shRNA+PD+T2DM groups than in the control group ($p < 0.001$, $p < 0.001$, $p < 0.001$, $p < 0.001$, $p < 0.001$, and $p < 0.01$, respectively). Furthermore, the total time was significantly shorter in the *IL-6R*-shRNA+PD+T2DM group relative to the PD+T2DM group ($p < 0.001$; Fig. 2A,B).

Analysis of Fasting Blood Glucose and Serum Insulin Levels

In mice that received MPTP (PD group), FBS levels did not increase significantly, whereas fasting serum insulin

Table 1. Real-time PCR primer sequences.

Gene	Forward (5′-3′), Reverse (3′-5′)
IL-6	CCACTCCCAACAGACCTGTC, GGTACTCCAGAAGACCAGAGG
IL-1β	GAAATGCCACCTTTTGACAGT, TGGATGCTCTCATCAGGACAG
TNF-α	CTGAACTTCGGGGTGATCG, GGCTTGTCACTCGAATTTTGAGA
IL-4	CCATATCCACGGATGCGACA, AAGCCCGAAAGAGTCTCTGC
HIF-1α	TCTCGGCGAAGCAAAGAGT, AGCCATCTAGGGCTTTCAGATAA
GAPDH	AGGTCGGTGTGAACGGATTTG, GGGGTCGTTGATGGCAACA

PCR, Polymerase Chain Reaction; IL, interleukin; *TNF-α*, tumor necrosis factor-α; *HIF-1α*, hypoxia-inducible factor-1α; *GAPDH*, Glyceraldehyde 3-phosphate dehydrogenase.

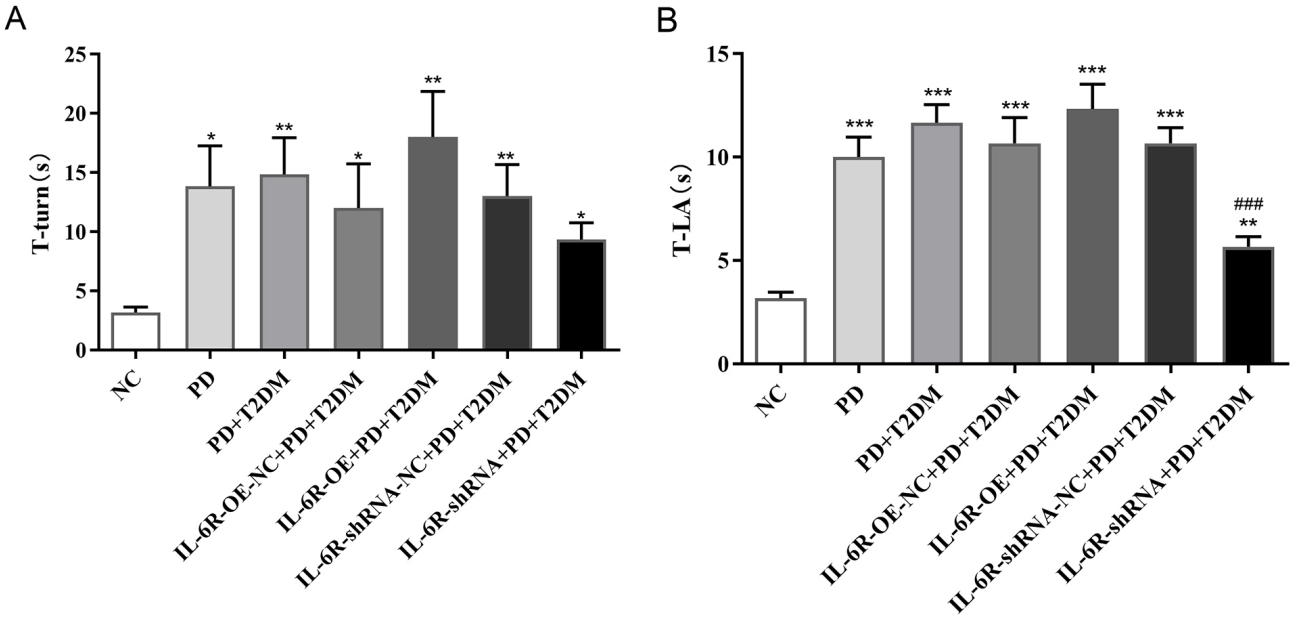

Fig. 2. Pole test. (A) Time of return, and (B) Total time. Number of parallel experiments, n = 6; *$p < 0.05$, **$p < 0.01$, ***$p < 0.001$ compared with the NC group; $^{###}p < 0.001$ in relative to the PD+T2DM group. PD, Parkinson's disease; T2DM, type 2 diabetes mellitus.

levels exhibited an obvious increase ($p < 0.05$). FBS and fasting serum insulin levels in the PD+T2DM group were shown to be markedly higher relative to those in the PD group ($p < 0.001$ and $p < 0.05$, separately) (Fig. 3A,B).

Impact of IL-6R Expression on Dopaminergic Neurons and α-Synuclein in Model Mice for Parkinson's Disease with Type 2 Diabetes as a Co-Morbidity

With the purpose of evaluating the effect of IL-6R on the nigrostriatal DA system, this study used western blotting to detect the level of TH and α-Synuclein in the SN. Compared with the control group, mice in the PD and PD+T2DM groups showed markedly decreased TH expression ($p < 0.05$ and $p < 0.001$, respectively) and elevated α-Synuclein deposition ($p < 0.05$, $p < 0.001$, respectively). Additionally, the PD+T2DM group exhibited lower TH expression ($p < 0.05$) and higher α-Synuclein deposition ($p < 0.05$) than the PD group. After injection of IL-6R-OE in the SN, these changes in TH and α-Synuclein were further aggravated ($p < 0.01$ and $p < 0.001$, respectively). However, the trends in TH and α-Synuclein were reversed with the administration of *IL-6R*-shRNA ($p < 0.05$ and $p < 0.05$, separately) (Fig. 4I–K). Consistent with the western blot findings, the immunofluorescence results showed similar trends in TH-positive neurons in the SN of each mouse group (Fig. 4A–H).

Impact of IL-6R Expression on the Microglial Cells in Mice with Parkinson's Disease with Type 2 Diabetes as a Co-Morbidity

As a marker of microglial activation, IBA-1 can be used for measuring the number of active microglial cells. We carried out immunofluorescence staining for IBA-1 and the results showed few activated microglial cells in the NC group. In the SN of PD and PD+T2DM mice, the levels of positive microglial staining were notably greater than those in the same areas in control mice ($p < 0.001$ and $p < 0.001$, respectively) (Fig. 5A–C), suggesting that microglia could be activated in the PD and PD+T2DM group mice. Further-

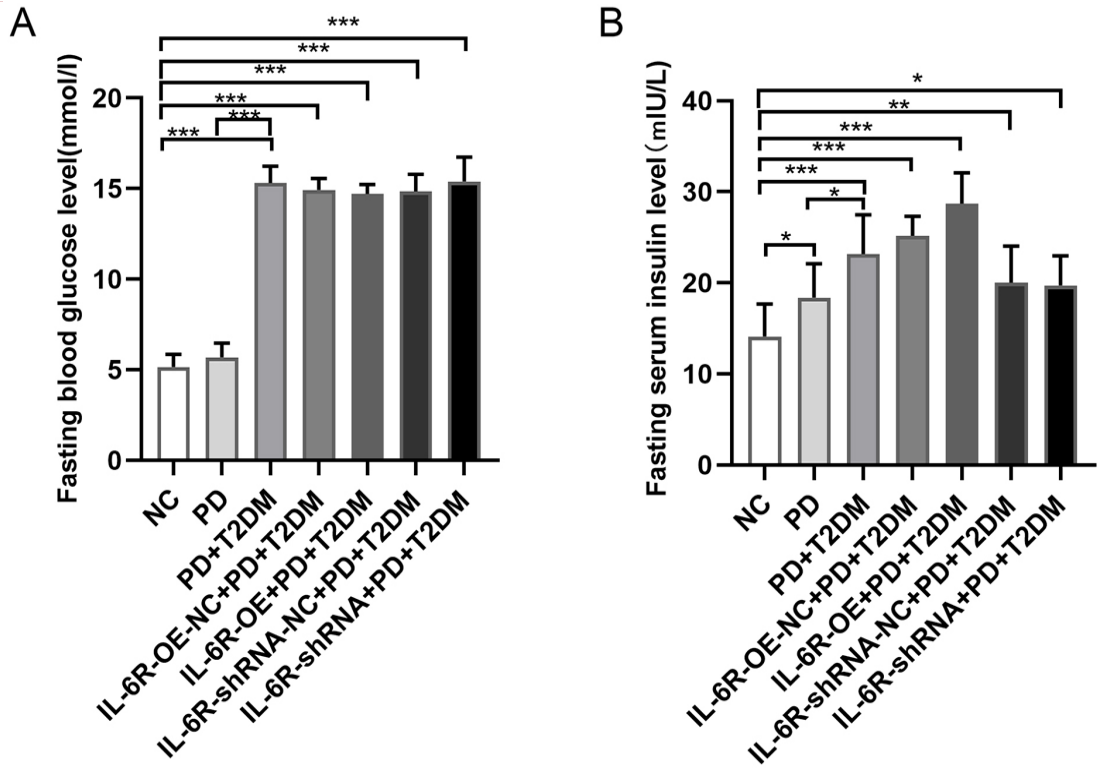

Fig. 3. Alteration of fasting blood glucose and serum Insulin in serum of mice. (A) Fasting blood glucose levels. (B) Fasting serum insulin levels in different groups. The number of parallel experiments was n = 10; *$p < 0.05$, **$p < 0.01$, ***$p < 0.001$.

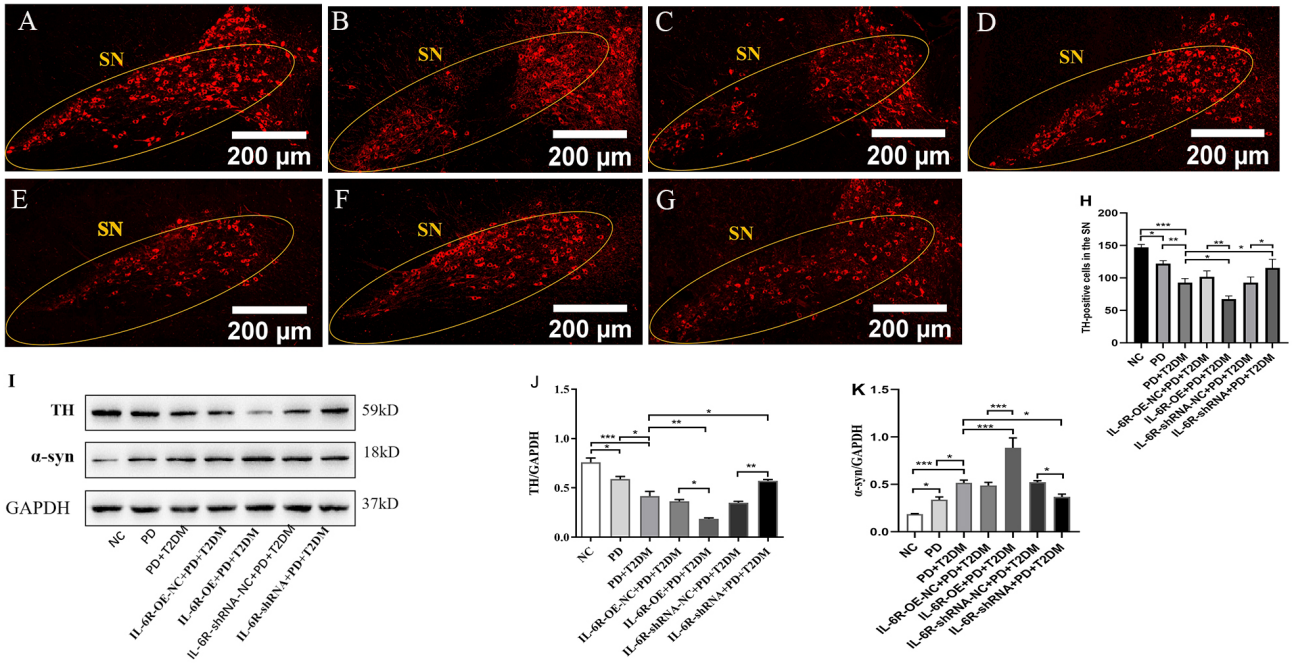

Fig. 4. Effects of IL-6R expression on dopaminergic neurons and α-Synucleinin the SN of mice in each group. (A–G) Representative micrographs of TH-stained dopaminergic neurons. (A) NC group, (B) PD group, (C) PD+T2DM group, (D) IL-6R-OE-NC+PD+T2DM group, (E) IL-6R-OE+PD+T2DM group, (F) *IL-6R*-shRNA-NC+PD+T2DM group, and (G) *IL-6R*-shRNA+PD+T2DM group. Scale bars: 200 μm. (H) The results for TH-positive cells are shown in histogram format. (I) Protein expression of TH and α-Synuclein for mice in various groups. (J,K) Analysis of TH and α-Synuclein protein expression. (Number of parallel experiments, n = 3.) *$p < 0.05$, **$p < 0.01$, ***$p < 0.001$. TH, tyrosine hydroxylase; SN, substantia nigra; IL-6R, IL-6 receptors.

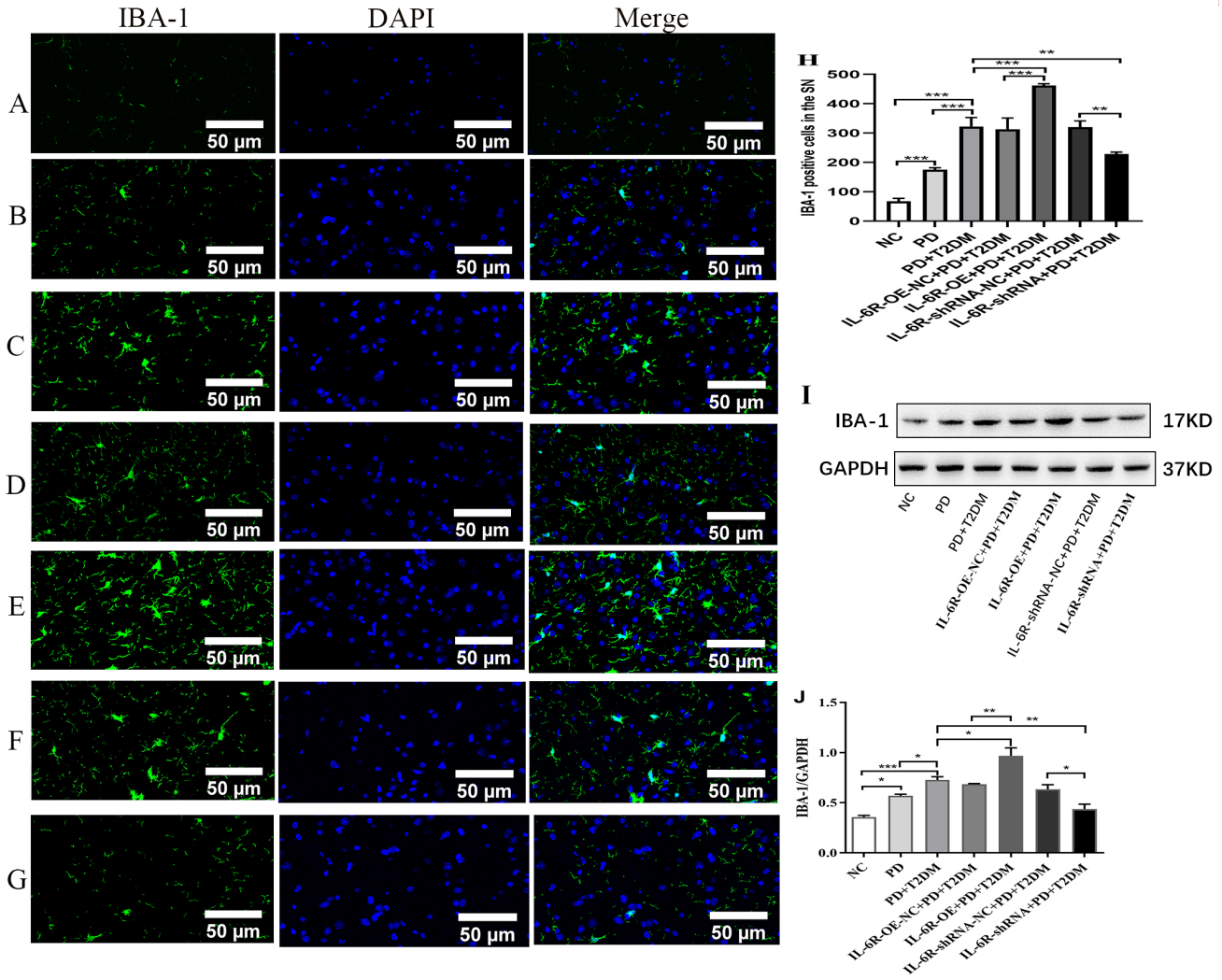

Fig. 5. Effects of IL-6R expression on the microglial cells in the SN of mice in each group. (A–G) Representative micrographs of immunofluorescence staining of IBA-1, DAPI, and merged images in the SN. (A) NC group, (B) PD group, (C) PD+T2DM group, (D) IL-6R-OE-NC+PD+T2DM group, (E) IL-6R-OE+PD+T2DM group, (F) *IL-6R*-shRNA-NC+PD+T2DM group, (G) *IL-6R*-shRNA+PD+T2DM group. Scale bars: 50 μm. (H) The results for IBA-1 positive cells in histogram format. (I) Protein expression of IBA-1 in different groups of mice. (J) Analysis of IBA-1 expression. (Number of parallel experiments, n = 3.) $*p < 0.05$, $**p < 0.01$, $***p < 0.001$. IBA-1, anti-ionized calcium-binding adaptor molecule 1.

more, the PD+T2DM group showed considerably higher IBA-1 expression than the PD group ($p < 0.001$). After the injection of IL-6R-OE into the SN, the expression of IBA-1 tended to increase further ($p < 0.001$). However, the expression of IBA-1 was reversed by *IL-6R*-shRNA administration ($p < 0.05$; Fig. 5D–H). Western blot analysis indicated the same trend for IBA-1 expression in the SN of each group of mice, consistent with the immunofluorescence staining results (Fig. 5I,J).

Effect of IL-6R Expression on Serum Inflammatory Cytokines TNF-α, IL-1β, IL-6, IL-4 and HIF-1α Levels in Parkinson's Disease Comorbid Type 2 Diabetes Mice

ELISA was carried out to identify the concentrations of HIF-1α and inflammatory cytokines like TNF-α, IL-1β, IL-6, and IL-4 in the serum of PD group mice and these factors were notably elevated in comparison with the NC group ($p < 0.01$, $p < 0.01$, $p < 0.05$, $p < 0.05$, $p < 0.01$, respectively). Obviously, the levels of TNF-α, IL-1β, and IL-6 in the PD+T2DM group were considerably elevated relative to that in the PD group ($p < 0.05$, $p < 0.05$, $p < 0.001$, respectively). Following intervention using IL-6R overexpression in the PD+T2DM group, the expression of TNF-α, IL-1β, IL-6, IL-4, and HIF-1α was further elevated ($p < 0.05$, $p < 0.05$, $p < 0.01$, $p < 0.05$, and $p < 0.05$, respectively). However, the opposite results were obtained for TNF-α, IL-1β, IL-6, IL-4, and HIF-1α after the intervention with *IL-6R*-shRNA in the PD+T2DM group ($p < 0.05$, $p < 0.05$, $p < 0.01$, $p < 0.05$, $p < 0.01$, separately) (Fig. 6A–E).

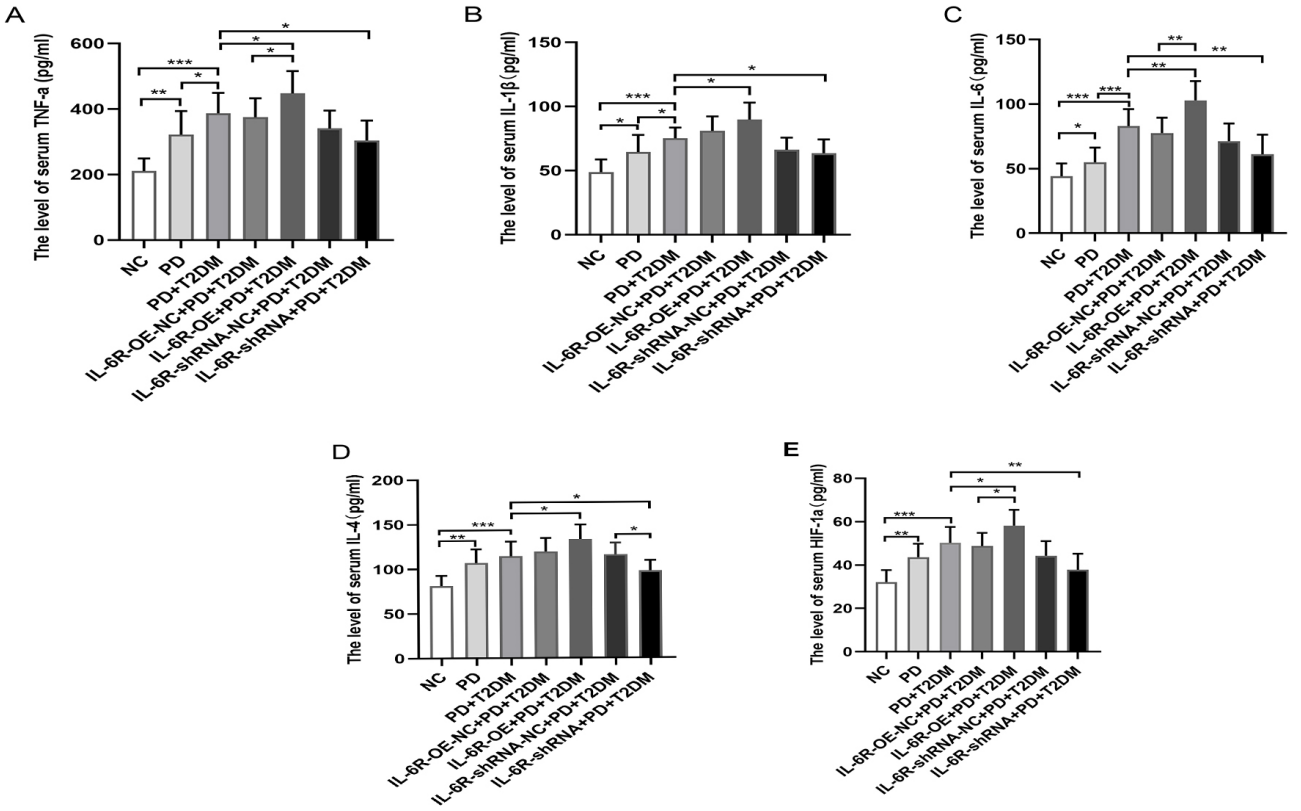

Fig. 6. Alteration of TNF-α, IL-1β, IL-6, IL-4 and HIF-1α in serum of mice. Serum levels of (A) TNF-α, (B) IL-1β, (C) IL-6, (D) IL-4, and (E) HIF-1α in each group of mice (Number of parallel experiments, n = 10.) *$p < 0.05$, **$p < 0.01$, ***$p < 0.001$.

IL-6R Expression Regulated the IL-6/STAT3/HIF-1α Signaling Pathway in Mice with Parkinson's Disease Comorbid Type 2 Diabetes

This study explored the activation of the STAT3/HIF-1α signaling pathway and phosphorylation of STAT3 (Tyr705) via western blotting to evaluate the downstream pathways of IL-6. Based on Fig. 6, MPTP administration triggered a remarkable increase in IL-6, IL-6R, p-STAT3 (Tyr705), and HIF-1α protein expression in the SN ($p < 0.05$, $p < 0.05$, $p < 0.001$, and $p < 0.05$, respectively). Hyperglycemia significantly increased the expression of these proteins, including IL-6, IL-6R, p-STAT3 (Tyr705), and HIF-1α ($p < 0.05$, $p < 0.05$, $p < 0.05$, and $p < 0.05$, respectively). Notably, injection of the IL-6R overexpression target gene further increased the expression of IL-6, IL-6R, p-STAT3 (Tyr705), and HIF-1α ($p < 0.01$, $p < 0.001$, $p < 0.05$, $p < 0.01$, respectively) in the Parkinson's disease comorbid type 2 diabetes mice. However, the injection of the *IL-6R*-shRNA target gene suppressed this increase ($p < 0.05$, $p < 0.01$, $p < 0.05$, and $p < 0.05$, respectively) (Fig. 7A–E).

Impact of IL-6R Expression on Inflammatory Cytokines TNF-α, IL-1β, IL-6, IL-4 and HIF-1α Levels in the SN in Parkinson's Disease Comorbid Type 2 Diabetes Mice

Using SN homogenates, we performed RT-qPCR, and the results suggested that the expressions of TNF-α, IL-1β, IL-6, IL-4, and HIF-1α in the PD group mice were markedly higher relative to those in NC mice ($p < 0.01$, $p < 0.01$, $p < 0.001$, $p < 0.001$, $p < 0.01$, respectively). Further, the levels of TNF-α, IL-1β, IL-6, and IL-4 in the PD+T2DM group exhibited an increase at levels greater than that in the PD group ($p < 0.05$, $p < 0.05$, $p < 0.01$, $p < 0.01$, respectively). Additionally, the level of TNF-α, IL-1β, IL-6, IL-4, and HIF-1α was further elevated after inducing IL-6R overexpression in the PD+T2DM group ($p < 0.001$, $p < 0.001$, $p < 0.001$, $p < 0.001$, $p < 0.001$, respectively). In comparison, the levels of TNF-α, IL-1β, IL-6, and HIF-1α were notably lower following administration of *IL-6R*-shRNA in the PD+T2DM group ($p < 0.01$, $p < 0.05$, $p < 0.001$, $p < 0.05$, separately) (Fig. 8A–E).

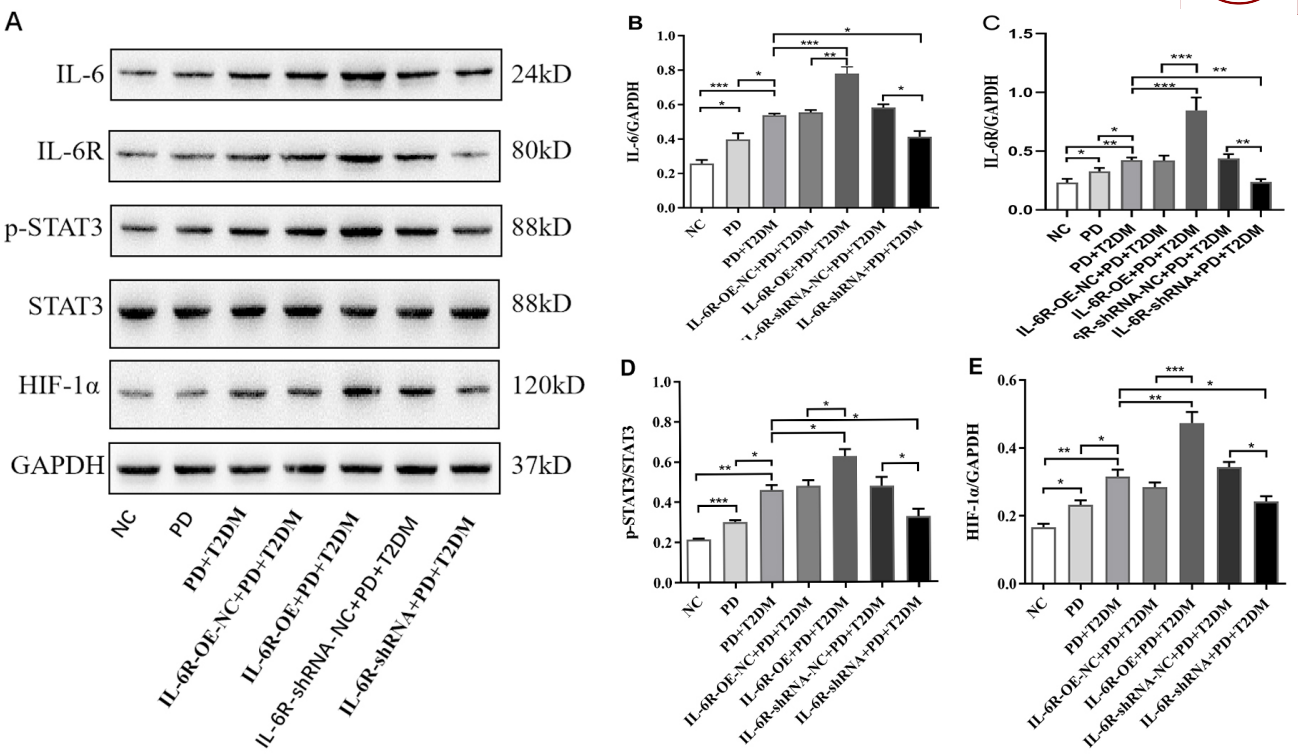

Fig. 7. Effects of IL-6R expression on the IL-6/STAT3/HIF-1α Signaling Pathway in the SN of mice in each group. (A) Expression of IL-6, IL-6R, p-STAT3 (Tyr705), STAT3, and HIF-1α in the SN. (B–E) Analysis of IL-6, IL-6R, p-STAT3 (Tyr705)/STAT3, and HIF-1α protein expression (Number of parallel experiments, n = 3.) $*p < 0.05$, $**p < 0.01$, $***p < 0.001$. STAT3, signal transducer and activator of transcription 3.

Discussion

Researchers are increasingly focusing on common inflammatory mechanisms between these two conditions owing to the rising incidence of PD and T2DM. In their study, Lee *et al.* [12] demonstrated that usnic acid hindered MPTP-induced dopaminergic neuronal loss and motor dysfunction by blocking NF-κB pathway activation in a PD mouse model. Peripheral and cerebral insulin-resistant mice fed an HFD showed disturbed IRS-1 phosphorylation and an elevated inflammatory response [13]. Hypoxia can aggravate inflammation, and emerging evidence suggests that hypoxia has a central impact on the pathological mechanisms associated with diabetes [14] and PD [15]. A key regulator of the hypoxia signaling pathway in inflammation is the HIF-1 factor. HIF-1 is a dimer which is consisted of two subunits (HIF-1α and HIF-1β). Based on conditions of normal oxygenation, HIF-1α has an extremely short half-life because it is continuously synthesized and degraded by the ubiquitin-proteasome system *de novo*. Based on hypoxic conditions, the proteasomal degradation and hydroxylation of the transcription factor HIF-1α were abrogated, protein expression of HIF-1α was elevated, and it translocates into the nucleus. Peng *et al.* [16] found that hypoxia could increase the level of the pro-inflammatory cytokines IL-1β, IL-6, and TNF-α, and the level of HIF-1α and NF-κB protein in BV2 microglia. Zhao *et al.* [17] demonstrated high glucose and hypoxia-induced HIF-1α up-regulation in human umbilical vein endothelial cells, whereas down-regulation of HIF-1α reduced inflammation and oxidative stress.

IL-6 refers to a multifunctional cytokine belonging to a subfamily of cytokines and is one of the main factors engaged in chronic subclinical inflammation. Physiologically, IL-6 is expressed in the macrophages, microglia, and neurons [18]. IL-6 receptors (IL-6R) are localized to microglia but not to oligodendrocytes or astrocytes [18]. IL-6 and IL-6R can accelerate chronic inflammation in the central nervous system, leading to PD progression [19]. Additionally, disruption of the BBB may result in the infiltration of inflammatory cells. IL-6 modulates BBB properties [19]. During signal transduction, IL-6 can first bind to the IL-6 receptor (IL-6R) subunit α. The IL-6/IL-6R complex is subsequently related to the transmembrane signal-transducing IL-6 receptor subunit β (gp130) and triggers gp130 dimerization [20]. IL-6 signaling induces the phosphorylation and nuclear localization of signal transducer and STAT3 by Janus kinase 2 (JAK2) [21]. Yang *et al.* [8] reported that echinacoside exerts neurotrophic and anti-inflammatory effects in MPTP-induced PD mice through regulation of the IL-6/JAK2/STAT3 pathway and phosphorylation of STAT3. Numerous studies have concentrated on evaluating the level of IL-6, STAT3, and HIF-1α in the inflammatory response of PD and T2DM. However, it

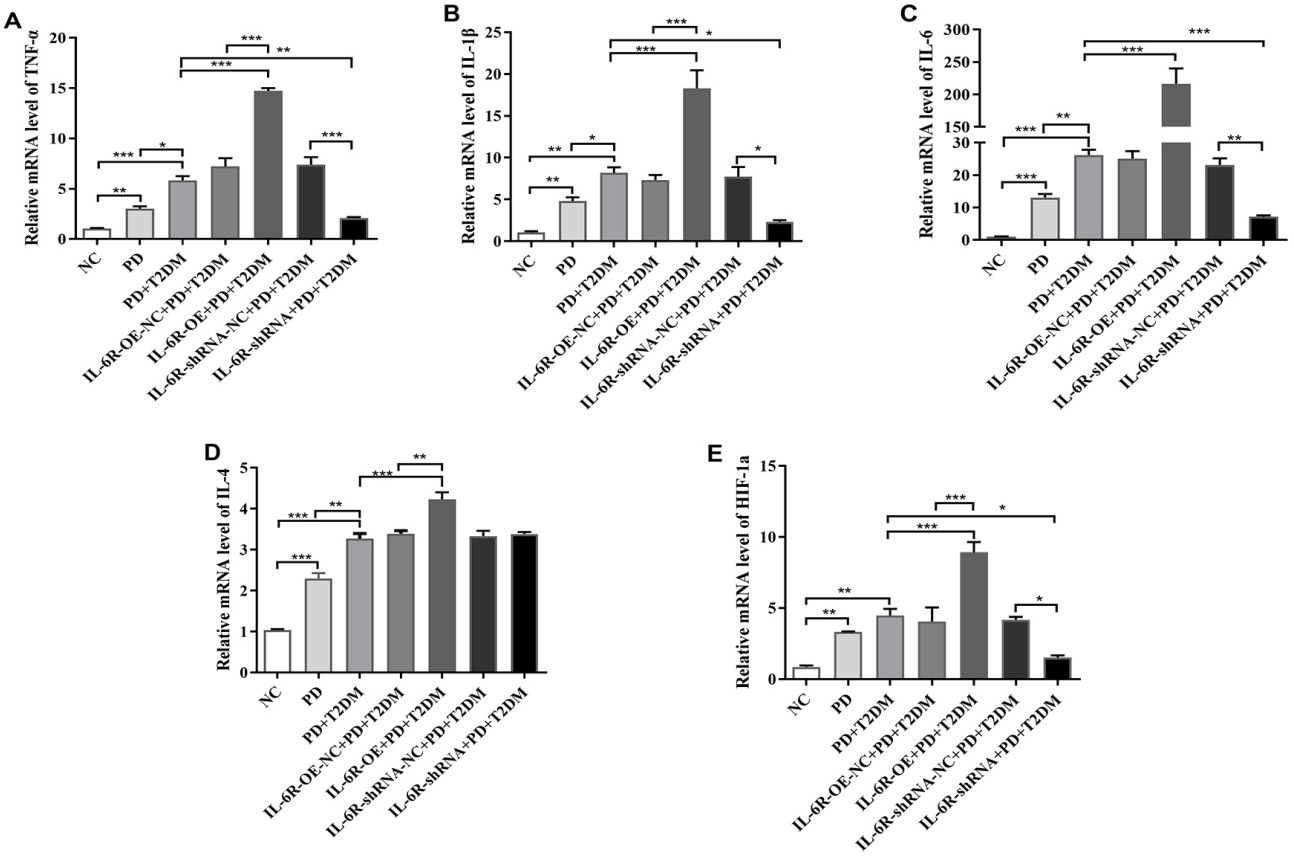

Fig. 8. Alteration of TNF-α, IL-1β, IL-6, IL-4 and HIF-1α in the SN of mice. Relative mRNA levels of (A) *TNF-α*, (B) *IL-1β*, (C) *IL-6*, (D) *IL-4* and (E) *HIF-1α* in the SN of different groups (Number of parallel experiments, n = 3.) $*p < 0.05$, $**p < 0.01$, $***p < 0.001$.

is unclear how the IL6/STAT3/HIF-1α signaling pathway functions in individuals undergoing PD with type 2 diabetes as a co-morbidity. In this work, we have constructed a mouse model of diabetes and Parkinson's disease as a co-morbidity and investigated whether IL-6R overexpression or the *IL-6R*-shRNA target gene silencing can mediate neuroinflammatory responses via the regulation of the IL-6/STAT3/HIF-1α signaling pathway.

Previously, it has been previously indicated that the incidence of abnormal glucose tolerance in PD patients can be as high as 50%–80% [22]. For a long time, insulin resistance has been a critical feature of T2DM. Recently, Hong *et al.* [3] demonstrated that insulin resistance can be found in the brains of patients undergoing PD. In our study, FBS levels in PD mice were slightly higher when compared with those in normal mice, with no statistical difference. This may be due to impaired glucose tolerance. The fasting serum insulin level in PD mice was notably higher than that in normal mice, indicating that insulin resistance may exist in PD mice. These results conform to those of the aforementioned studies. Although co-morbidity appeared to enhance motor defects in the pole test when compared to PD mice, the results of statistical analysis exhibited no obvious difference between the PD and PD+T2DM groups, suggesting that hyperglycemia did not affect the severity of PD. By contrast, Pérez *et al.* [23] found that diabetes aggravated oxidative stress in the striatum, altered dopamine neurotransmission, and enhanced the susceptibility to neurodegenerative injuries that cause movement disorders. This may be explained by the fact that in our model, MPTP severely aggravated motor dysfunction and may have masked the impact of high glucose levels on motor function.

Wang *et al.* [24] indicated increased expression of pro-inflammatory cytokines TNF-α, IL-6, and IL-1β in MPTP-treated db/db mice. This result is consistent with the findings of this study, which suggests that T2DM can accelerate neuroinflammation in PD. Yang *et al.* [8] demonstrated that activation of the IL-6/JAK2/STAT3 pathway could activate the microglia, damage DA neurons, and elevate the levels of inflammatory cytokines TNF-α, IL-1β, and IL-6 in PD mice. This was similar to our findings. In addition, we found that in PD with T2DM co-morbid mice, these changes were further aggravated. Yang *et al.* [8] also showed that with the IL-6/JAK2/STAT3 pathway being inhibited, the number of damaged dopamine neurons increased and the expression of inflammatory markers decreased. Lin *et al.* [25] reported that the inhibition of

the JAK2/STAT3/HIF-1α signaling pathway resulted in reduced transcription of HIF-1α in SH-SY5Y neuroblastoma cells co-cultured with pathological α-Synuclein-induced human microglial clone 3 (HMC3) cells. The significant reduction in pro-inflammatory cytokines found in this study may result due to inhibition of the IL-6/STAT3/HIF-1α signaling pathway. Furthermore, injection of the *IL-6R*-shRNA target gene in the SN in the PD with T2DM comorbid mice lowered the expression of IL-6, p-STAT3, HIF-1α, and the microglia activation marker IBA-1, and increased the expression of dopamine neuron-specific marker TH. However, inhibition of the IL-6/STAT3/HIF-1α pathway may not influence the activation of astrocytes. Qin *et al*. [26] showed that no significant changes in the expression of Glial fibrillary acidic protein (GFAP), an astrocyte marker, were observed when the JAK/STAT pathway was inhibited.

This work is the first attempt to explore the inflammatory mechanism underlying the development of PD with T2DM as a co-morbidity via the IL-6/STAT3/HIF-1α signaling pathway. Nevertheless, the present study has a few limitations. First, we did not set up a separate group for T2DM. The effects of IL-6R expression on the IL-6/STAT3/HIF-1α signaling pathway in diabetic mice were not observed. Second, we did not perform the pole test on all mice. The return time was unchanged by the shRNA. A larger sample size such as 12 or 15 mice per group would be required in future studies, to check if shRNA treatment shortens the return time. Additionally, the hypothesis that blocking IL-6 signaling may act as a rational treatment for neuroinflammatory and metabolic inflammatory diseases may require further testing. Tocilizumab, a monoclonal antibody against IL-6R, binds to membrane-bound and soluble IL-6R, thereby blocking the binding of IL-6 [18]. Although the application of tocilizumab in treating Parkinson's disease is rarely reported, tocilizumab has been shown to protect against diabetic kidney injury by improving insulin resistance and inhibiting the inflammasome in db/db mice [27].

Conclusions

To conclude, our study provides solid evidence that PD comorbid with T2DM progression can be boosted by AAV-mediated IL-6R overexpression, which upregulates the IL-6/STAT3/HIF-1α pathway. In contrast, AAV *IL-6R*-shRNA treatment suppresses the IL-6/STAT3/HIF-1α pathway, reduces neuroinflammation, and protects dopamine neurons, thus weakening the development of PD comorbid with T2DM. Thus, IL-6R inhibition may serve as an underlying molecular target for targeting PD with T2DM as a co-morbidity.

Availability of Data and Materials

The datasets used and analyzed to support the findings of this study are available from the first author upon request.

Author Contributions

AH, YZ, YS and YW made substantial contributions to conception and design. RL and JW made substantial contributions to the acquisition of data. XC, LY and HJ made substantial contributions to the analysis and interpretation of data. AH, RL, JW, XC, LY and HJ have been involved in drafting the manuscript. YZ, YW and YS have been involved in revising the manuscript critically for important intellectual content. All authors also have given final approval of the version to be published and agreed to be accountable for all aspects of the work.

Ethics Approval and Consent to Participate

The animals were subject to treatment based on the instructions specified in the revised Animals (Scientific Procedures) Act 1986 in the UK. The experimental protocols were approved by the Experimental Animal Ethics Committee of the Nanjing University of Chinese Medicine (ethical approval number: ACU220604).

Acknowledgment

We are grateful for the language editing service by Editage company.

Funding

This work was supported by the Jiangsu Province Chinese Medicine Leading Talent Project (No. SLJ0214) and the Nanjing Pukou District Social Enterprise Science and Technology Development Plan Project (S2022-3) for financial support.

Conflict of Interest

The authors declare no conflict of interest.

Supplementary Material

Supplementary material associated with this article can be found, in the online version, at https://doi.org/10.24976/Discov.Med.202436186.129.

References

[1] Venkatesan D, Iyer M, S RW, Narayanasamy A, Kamalakannan S, Valsala Gopalakrishnan A, *et al*. Genotypic-Phenotypic Analysis, Metabolic Profiling and Clinical Correlations in Parkinson's Disease Patients from Tamil Nadu Population, India. Journal of Molecular Neuroscience: MN. 2022; 72: 1724–1737.

[2] Chow EYK, Chan JCN. Insulin resistance versus β-cell dysfunction in type 2 diabetes: where public and personalised health meet. The Lancet. Diabetes & Endocrinology. 2020; 8: 92–93.

[3] Hong CT, Chen KY, Wang W, Chiu JY, Wu D, Chao TY, *et al*. Insulin Resistance Promotes Parkinson's Disease through Aberrant Expression of α-Synuclein, Mitochondrial Dysfunction, and Deregulation of the Polo-Like Kinase 2 Signaling. Cells. 2020; 9: 740.

[4] Cheong JLY, de Pablo-Fernandez E, Foltynie T, Noyce AJ. The Association Between Type 2 Diabetes Mellitus and Parkinson's Disease. Journal of Parkinson's Disease. 2020; 10: 775–789.

[5] Rajchgot T, Thomas SC, Wang JC, Ahmadi M, Balood M, Crosson T, *et al*. Neurons and Microglia; A Sickly-Sweet Duo in Diabetic Pain Neuropathy. Frontiers in Neuroscience. 2019; 13: 25.

[6] Liu M, Gao L, Zhang N. Berberine reduces neuroglia activation and inflammation in streptozotocin-induced diabetic mice. International Journal of Immunopathology and Pharmacology. 2019; 33: 2058738419866379.

[7] Van Dyken P, Lacoste B. Impact of Metabolic Syndrome on Neuroinflammation and the Blood-Brain Barrier. Frontiers in Neuroscience. 2018; 12: 930.

[8] Yang X, Yv Q, Ye F, Chen S, He Z, Li W, *et al*. Echinacoside Protects Dopaminergic Neurons Through Regulating IL-6/JAK2/STAT3 Pathway in Parkinson's Disease Model. Frontiers in Pharmacology. 2022; 13: 848813.

[9] Yu T, Sungelo MJ, Goldberg IJ, Wang H, Eckel RH. Streptozotocin-Treated High Fat Fed Mice: A New Type 2 Diabetes Model Used to Study Canagliflozin-Induced Alterations in Lipids and Lipoproteins. Hormone and Metabolic Research = Hormon- Und Stoffwechselforschung = Hormones et Metabolisme. 2017; 49: 400–406.

[10] Hassanzadeh K, Rahimmi A, Moloudi MR, Maccarone R, Corbo M, Izadpanah E, *et al*. Effect of lobeglitazone on motor function in rat model of Parkinson's disease with diabetes co-morbidity. Brain Research Bulletin. 2021; 173: 184–192.

[11] Chen C, Xia B, Tang L, Wu W, Tang J, Liang Y, *et al*. Echinacoside protects against MPTP/MPP^+-induced neurotoxicity via regulating autophagy pathway mediated by Sirt1. Metabolic Brain Disease. 2019; 34: 203–212.

[12] Lee S, Lee Y, Ha S, Chung HY, Kim H, Hur JS, *et al*. Anti-inflammatory effects of usnic acid in an MPTP-induced mouse model of Parkinson's disease. Brain Research. 2020; 1730: 146642.

[13] Subba R, Sandhir R, Singh SP, Mallick BN, Mondal AC. Pathophysiology linking depression and type 2 diabetes: Psychotherapy, physical exercise, and fecal microbiome transplantation as damage control. The European Journal of Neuroscience. 2021; 53: 2870–2900.

[14] Catrina SB, Zheng X. Hypoxia and hypoxia-inducible factors in diabetes and its complications. Diabetologia. 2021; 64: 709–716.

[15] Bhatia D, Ardekani MS, Shi Q, Movafagh S. Hypoxia and its Emerging Therapeutics in Neurodegenerative, Inflammatory and Renal Diseases. Hypoxia and Human Diseases. 2017; 21: 404–443.

[16] Peng X, Li C, Yu W, Liu S, Cong Y, Fan G, *et al*. Propofol Attenuates Hypoxia-Induced Inflammation in BV2 Microglia by Inhibiting Oxidative Stress and NF-κB/Hif-1α Signaling. BioMed Research International. 2020; 2020: 8978704.

[17] Zhao M, Wang S, Zuo A, Zhang J, Wen W, Jiang W, *et al*. HIF-1α/JMJD1A signaling regulates inflammation and oxidative stress following hyperglycemia and hypoxia-induced vascular cell injury. Cellular & Molecular Biology Letters. 2021; 26: 40.

[18] Rothaug M, Becker-Pauly C, Rose-John S. The role of interleukin-6 signaling in nervous tissue. Biochimica et Biophysica Acta. 2016; 1863: 1218–1227.

[19] Ma J, Gao J, Niu M, Zhang X, Wang J, Xie A. P2X4R Overexpression Upregulates Interleukin-6 and Exacerbates 6-OHDA-Induced Dopaminergic Degeneration in a Rat Model of PD. Frontiers in Aging Neuroscience. 2020; 12: 580068.

[20] Akbari M, Hassan-Zadeh V. IL-6 signalling pathways and the development of type 2 diabetes. Inflammopharmacology. 2018; 26: 685–698.

[21] Xu S, Yu C, Ma X, Li Y, Shen Y, Chen Y, *et al*. IL-6 promotes nuclear translocation of HIF-1α to aggravate chemoresistance of ovarian cancer cells. European Journal of Pharmacology. 2021; 894: 173817.

[22] Marques A, Dutheil F, Durand E, Rieu I, Mulliez A, Fantini ML, *et al*. Glucose dysregulation in Parkinson's disease: Too much glucose or not enough insulin? Parkinsonism & Related Disorders. 2018; 55: 122–127.

[23] Pérez-Taboada I, Alberquilla S, Martín ED, Anand R, Vietti-Michelina S, Tebeka NN, *et al*. Diabetes Causes Dysfunctional Dopamine Neurotransmission Favoring Nigrostriatal Degeneration in Mice. Movement Disorders: Official Journal of the Movement Disorder Society. 2020; 35: 1636–1648.

[24] Wang L, Zhai YQ, Xu LL, Qiao C, Sun XL, Ding JH, *et al*. Metabolic inflammation exacerbates dopaminergic neuronal degeneration in response to acute MPTP challenge in type 2 diabetes mice. Experimental Neurology. 2014; 251: 22–29.

[25] Lin D, Zhang H, Zhang J, Huang K, Chen Y, Jing X, *et al*. α-Synuclein Induces Neuroinflammation Injury through the *IL6ST-AS*/STAT3/HIF-1α Axis. International Journal of Molecular Sciences. 2023; 24: 1436.

[26] Qin H, Buckley JA, Li X, Liu Y, Fox TH, 3rd, Meares GP, *et al*. Inhibition of the JAK/STAT Pathway Protects Against α-Synuclein-Induced Neuroinflammation and Dopaminergic Neurodegeneration. The Journal of Neuroscience: the Official Journal of the Society for Neuroscience. 2016; 36: 5144–5159.

[27] Wu R, Liu X, Yin J, Wu H, Cai X, Wang N, *et al*. IL-6 receptor blockade ameliorates diabetic nephropathy via inhibiting inflammasome in mice. Metabolism: Clinical and Experimental. 2018; 83: 18–24.